NASA-CR-197099

P-14

FINAL REPORT FOR UMIS

Ultraviolet-Infrared Mapping Interferometric Spectrometer

NAGW-2423 Start: 1 January, 1991 End: 28 February, 1994

SUMMARY

Prism and grating spectrometers have been the defacto devices for spectral mapping and imaging (hereafter referred to as hyperspectra). We have developed a new, hybrid instrument with many superior capabilities, the Digital Array Scanned Interferometer, DASI. The DASI performs the hyperspectral data acquisition in the same way as a grating or prism spectrograph, but retains the substantial advantages of the two-beam (Michelson) interferometer with additional capabilities not possessed by either of the other devices. The DASI is capable of hyperspectral studies in virtually any space or surface environment at any wavelength from below 50 nm to beyond 12 microns with available array detectors.

By our efforts, we have defined simple, low cost, no-moving parts DASIs capable of carrying out hyperspectral science measurements for solar system exploration missions, e.g. for martian, asteroid, lunar, or cometary surveys. DASI capabilities can be utilized to minimize cost, weight, power, pointing, and other physical requirements while maximizing the science data return for spectral mapping missions. Our success in the development of DASIs has become and continues to be an important influence on the efforts of the best research groups developing remote sensing instruments for space and other applications.

Accomplishments

During the UMIS project, we have completed all proposed components of the UMIS development. Beginning on 1 January, 1991, we implemented the NICMOS SWIR arrays, funded under PIDDP auspices. These arrays were essential for the science measurements in the important mineralogical spectral region from 0.8 to 2.5 μm. We received an engineering grade 256x256 SWIR (NICMOS III) array from Rockwell in March, 1991 that allowed us to complete a design for, build, and test a pc-based portable detector control and data acquisition system, define dewar configurations, and program software for image acquisition and storage. Those major efforts realized the full operation of the NICMOS III for the demonstration of the DASI capabilities for UMIS' science measurement goals.

We received a near-science quality NICMOS III array in July, 1991 whereupon we initiated tests of NICMOS III using the newly completed electronic data acquisition system, as described above. Subsequently, we have received two science grade NICMOS III arrays to complete our acquisition of the SWIR array detectors. These devices have provided excellent DASI spectral data for many circumstances since their implementation. We were among the first university groups to implement NICMOS III arrays fully and have thus made an effort to document the time variability of the NICMOS III array.

The NICMOS III arrays were characterized, especially for the fast read rates required for observations of bright solar system objects such as Mars, the Moon, or for Mission to Earth applications. UMIS require

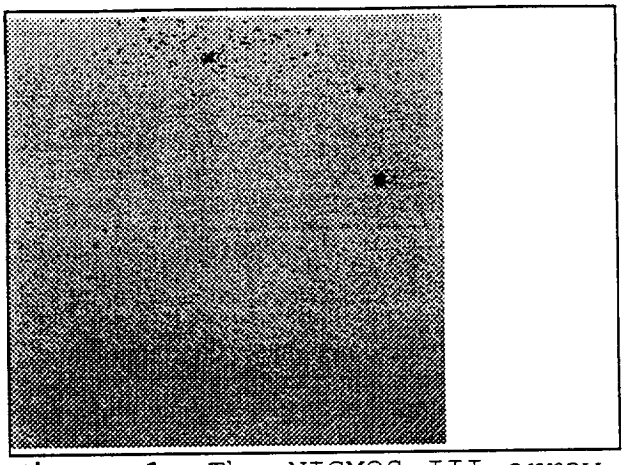

Figure 1. The NICMOS III array, illuminated by white light, shows the pixel defects.

requirements place significant demands upon the readout capability of NICMOS III arrays. Most baseline missions (as well as the Lumis Scout mission briefly described below) require a frame read time of a few hundred milliseconds with acceptable read noise, dynamic range and other properties. With our data system, we can achieve read rates of 350 milliseconds per frame with no compromise of the NICMOS III parameters and 200 milliseconds with a moderate read noise increase. It is possible to increase this rate to 10 Hz or more with the NICMOS III multiplexer while recent advances in the multiplexer design permit even higher rates with increased well depths. These rates are easily fast enough and the increased well depths sufficient for all probable UMIS science measurements, including many Earth missions. A much faster, larger well depth SWIR array is available for reaching very high S/N, i.e. over 1000 and for longer wavelength operation to as long as 10.5 μm at 77K.

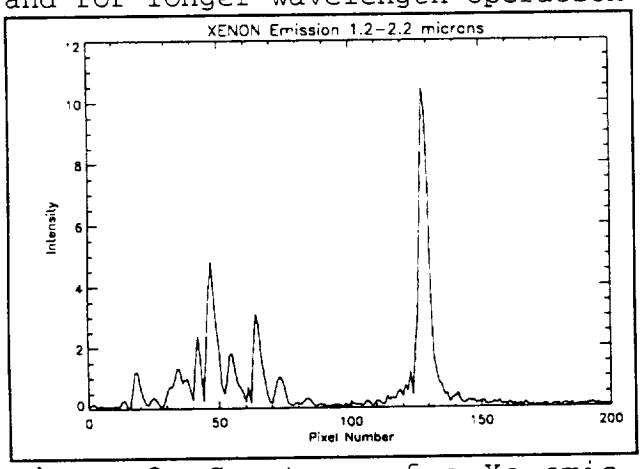

Figure 2. Spectrum of a Xe emission lamp between 1.2 and 2.2 μm.

A NICMOS III flat field image is displayed in Figure 1, showing the pixel defects. That particular device had over 99.6% good pixels and a quantum efficiency at 2.35 μm of over 65%. This NICMOS III device has shown aging effects. The device aging is shown primarily in haloes that appeared around many of the single pixel defects. There was a modest erosion in the number of good pixels in the two year interval. This characteristic makes it essential that an accurate method of on-board calibration be available if the NICMOS III is to be used for long duration space missions.

With the near-science grade NICMOS III device, we began laboratory and field spectroscopy to define the capabilities of NICMOS III arrays in the context of DASI observations. The first tests were intended to obtain spectra of a known source and thereby calibrate the wavelength response of NICMOS III and determine the spectral fidelity of the DASI in the near IR. We acquired interferograms with laboratory sources to accomplish this goal. An example calibration spectrum from a Xe arc source is shown in Figure 2. The known spectral lines from such lamps offer a simple means to acquire calibrations for extended space missions.

DASI Fourier Transform Analysis Procedures

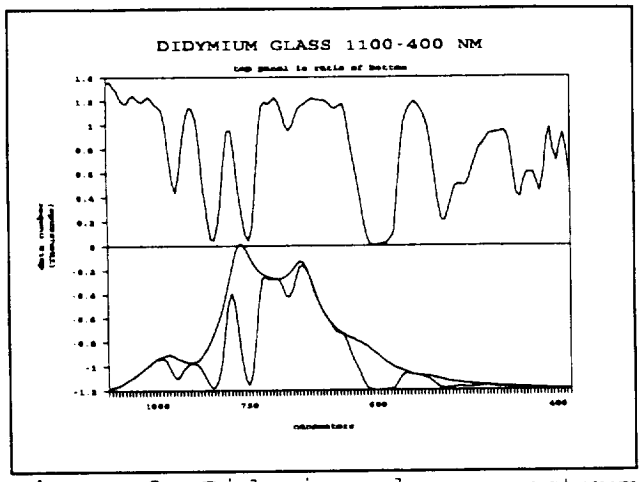

Figure 3. Didymium glass spectrum standard obtained with DASI.

Procedures for reducing the acquired interferograms were written and called from within IDL to handle FITS images, provide the Fast Fourier Transform and the means to display, and print the results (TIF and PS formats, primarily). The analysis includes the computation of mean wavelength images and other useful processing modes to display and catalogue the data. We took care to check that our spectral analysis yielded a spectral product consistent with known spectra. An example laboratory spectrum of a calibration medium, didymium glass, is shown in Figure 3. The lower panel is the instrument profile with and without the didymium glass. The upper panel is their divisor, yielding an accurate didymium spectrum.

The interferogram processing consists of removing detector and illumination effects, taking account of the finite number and width of interferogram samples, and then use interferogram phase information to obtain an accurate symmetrization of the interferogram and finally computing a spectral estimate with an optimized FFT method. For the birefringent UMIS design, polarization is also taken into account. These procedures are integrated into a fast, easily usable method for data acquisition and analysis with DASIs. As we continue to utilize DASIs for diverse applications, as described below, we expect to evolve data analysis procedures optimized for the specific spectral characteristics of the observed sources.

Birefringent DASI Studies

The proposed birefringent DASI introduces polarization as an instrument parameter. Source polarization can generally influence the spectral output and has been included in the ray trace and interference analysis of the optical system for UMIS to define the entire system in terms of its interferometric and optical properties. The birefringent interferometer permits the acquisition of in- and out-of-phase interferograms that remove most of the continuum contribution to the interferogram and the pixel-to-pixel effects of the detector arrays.

We have used the birefringent DASI prototype to acquire many results to demonstrate its properties in the lab and in the field. The birefringent DASI provides high contrast in the interferogram, as high as 87% has been measured. This is due in part to the use of a Wollaston prism which generally operates with nearly constant efficiency over the entire response range of the CCD, NICMOS III, or other infrared arrays. The Wollaston prism is a nearly perfect beam splitter. Interferograms with an high contrast yield superior signal-to-noise in the Fourier transform spectra.

Heritage of the Method

Smith (1990), Smith and Schempp (1991), and Smith and Smith (1994) describe the nature of hyperspectra in the context of digital array scanned interferometers. Smith (1990) originally conceived the DASI as an instrument with which to acquire spectral image cubes in the same mode as a grating or prism spectrometer while retaining the advantages of two-beam interferometers. The key DASI component is the modern digital array detector that permits the acquisition of high dynamic range interferograms in a digital form amenable to the rapid computation of Fourier transforms. The available two dimensional arrays provide a dynamic range exceeding 10,000 and provide for the use of the redundant interferogram coordinate to obtain spatially resolved spectra. Infrared array detector technology has extended the photon noise limited regime out to 2.5 μm or beyond. DASI advantages arising from Fourier transform spectroscopy include the optimum instrument profile, an étendue not limited by the resolution-luminosity product, insensitivity to parasitic or stray light, and an high overall efficiency for very broad spectral regions. The DASI is thus a cost-effective replacement for grating or prism spectrometers for the acquisition of spectral image cubes.

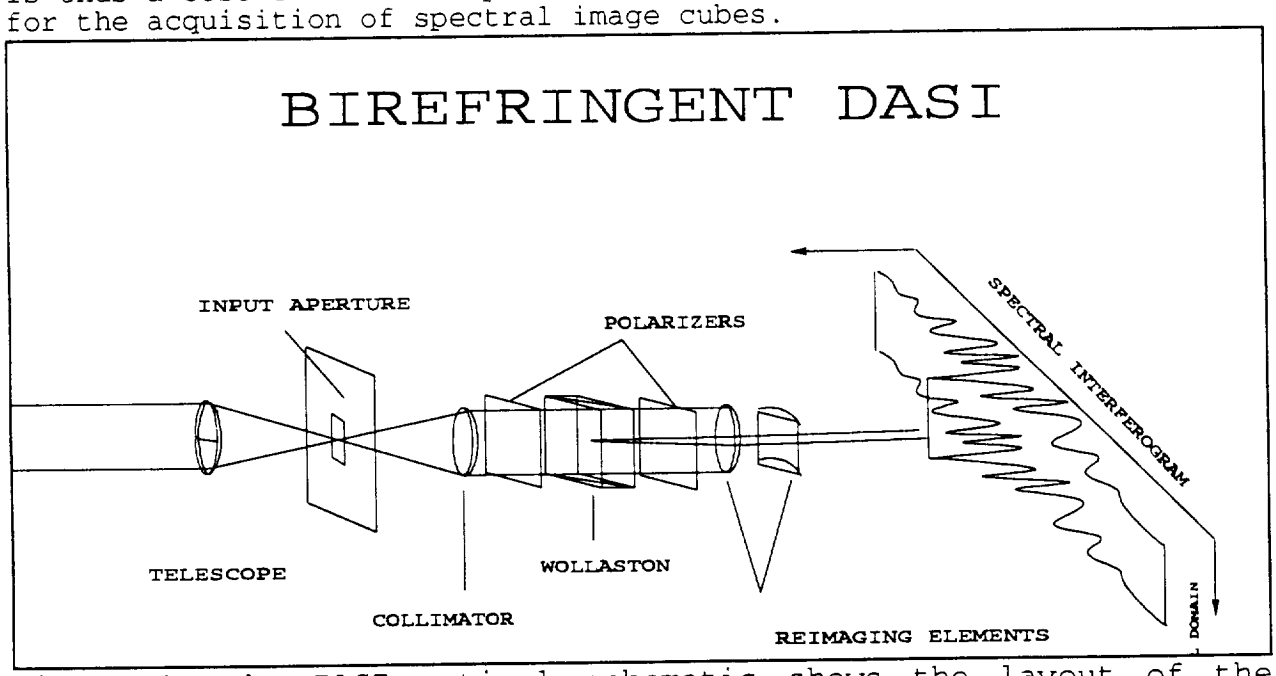

Figure 1. The DASI optical schematic shows the layout of the essential elements, as used in DASI prototypes to acquire hyperspectral data.

THE DIGITAL ARRAY SCANNED INTERFEROMETER

The DASI is constructed around a birefringent Digital Array Scanned Interferometer. The interferometer optics are schematically shown in Figure 4. Smith and Schempp (1991), Smith and Smith (1994), and Okamoto et al.(1986)) have described related instruments. The DASI acquires all spectral elements in a spectrally "multiplexed" mode while the spectral and one spatial dimension are acquired in a "multichannel" mode as with

a grating or prism spectrometer. The second spatial dimension is pushbroom mapped. The rigid, solid state construction of DASI renders it inherently insensitive to vibrations and thermal effects, and based on results quoted herein, is well suited for remote, unattended operation, as required for robotic missions planned in the inner and outer solar system.

The observed interferogram is a discrete sampling of the continuous interferogram. An interferogram cannot be sampled to infinity, but is truncated at a finite value of x, so that the total number, N, of points in a symmetrically sampled interferogram is less than or equal to the pixel length of the array detector. The interferogram encodes all frequencies (wavelengths in cm^{-1}) up to σ_{max} when we sample with $\beta/\phi = 2d\sigma_{max}$, corresponding to a spectral resolution of $\delta\sigma = \beta/d\phi N$, where N is the number of pixels. β and ϕ are the magnification and shearing angle, respectively. The spatial sampling of the interferogram divides the incident flux over the N pixels of the detector. Location of the central maximum and symmetrization of the interferogram usually require that the number of samples be 10-20% less than the detector pixel count. Since an interferogram is spatially sampled for all elements at once, DASI is inherently insensitive to variations in the incident flux over the integration interval, i.e. a multichannel detector in wavenumber.

Motivation for the DASI Instrument

Spectral spatio-temporal variations are complex in real geochemical systems (bio- effects are included in the role of hyperspectral measurement of the Earth from space platform) and must be measured accurately with high precision to attain a unique response. Generally, a greater the number of sampled spectral elements provides a greater constraint on the identifications and quantitative interpretations of (bio-) geochemical composition. The maximum constraint on spectral identifications and abundance measurements, then, is achieved where all relevant wavelengths are simultaneously measured with high photometric accuracy over a broad selectable spectral region. The DASIs defined herein are aimed at the optimization of the above stated science measurement goals.

DASI Advantageous Characteristics

A major DASI advantage is that it provides the simple operational characteristics of grating or prism spectrometers for spectral imaging while retaining the highly desirable characteristics of two-beam interferometers in terms of throughput, spectral fidelity, and response.

A DASI encodes each wavelength in the incident spectrum so that parasitic and stray light are not reconstructed in the spectrum. Only the ac component of the interferogram contributes in the reconstruction. This allows the establishment of a well defined continuum and provides for more quantitative spectral analyses. AC only sensitivity is an inherent advantage for DASIs compared to spectral dispersing instruments where light falling on the array detector pixels at the position of strong absorption features is contaminated by stray and/or scattered light that cannot be differentiated from the desired light. The attained photometric accuracy for grating instruments is a function of the stray and parasitic light, detector dark current, read noise, and pixel-to-pixel wavelength response variations. Consequently, the highest accuracy data has been acquired with two-beam interferometers of which a DASI is a variant.

A DASI's instrumental profile is the sinc function that has the favorable characteristic of an equal response to all frequencies up to its cutoff, σ_{max}, with the modification noted by Smith and Schempp (1991). By comparison, a grating spectrometer normally has a triangular instrument function that strongly attenuates the higher spatial frequencies. Smith and Smith (1994), following Ring and Stevens (1972), show that spectral profiles measured with DASI, like other two beam interferometers, can achieve better effective spectral resolution than grating spectrometers at a specified spectral resolving power. To achieve the same measured spectral response, a DASI requires as few as one-third the number of measured spectral elements as a grating or prism spectrograph. Consequently, up to 3X higher flux per pixel can illuminate the detector compared with an equivalent spectral resolving power grating monochromator, improving the S/N achievable with DASI in a given observational circumstance, irrespective of other characteristics.

Smith and Smith (1994), following Jacquinot (1954), have compared an interferometer's étendue and resolution-luminosity product, $R\Omega$, with an equivalent aperture and spectral resolution grating spectrometer (GRMS) as used in spectral mapping. This analysis gives a lower limit to DASI's étendue since it is not constrained by the resolution-luminosity product. The spatial resolution across the aperture of DASI is determined only by the imaging requirements. Smith (1990) showed that a cylindrical lens that images the entrance aperture onto the array in the vertical (redundant) dimension allows spatially resolved spectra to be acquired simultaneously. Pushbroom scanning of the DASI entrance aperture across a scene yields hyperspectra for the observed scene.

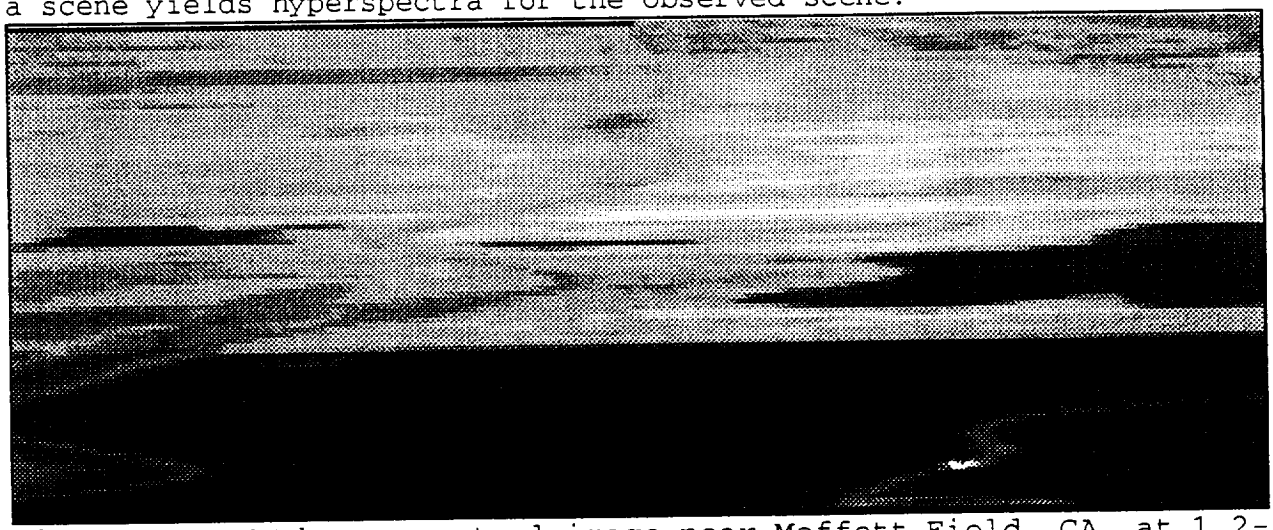

Figure 5. DASI hyperspectral image near Moffett Field, CA. at 1.2-2.2 μm, obtained from C130 at 5x20 meter spatial resolution. The dark areas are mostly tidal flats.

DASI OBSERVATIONAL DATA

Since DASIs cannot first be used on spacecraft, airborne hyperspectra with our existing DASI have been acquired to verify in detail the above concepts. Figure 5 is an airborne DASI pushbroom scanned infrared (mean wavelength of 1.6 μm) spectral image acquired during a C130 flight, shown as an example of our prototype DASI;s ability to provide spectral information for scanned fields of view. This spectral image has

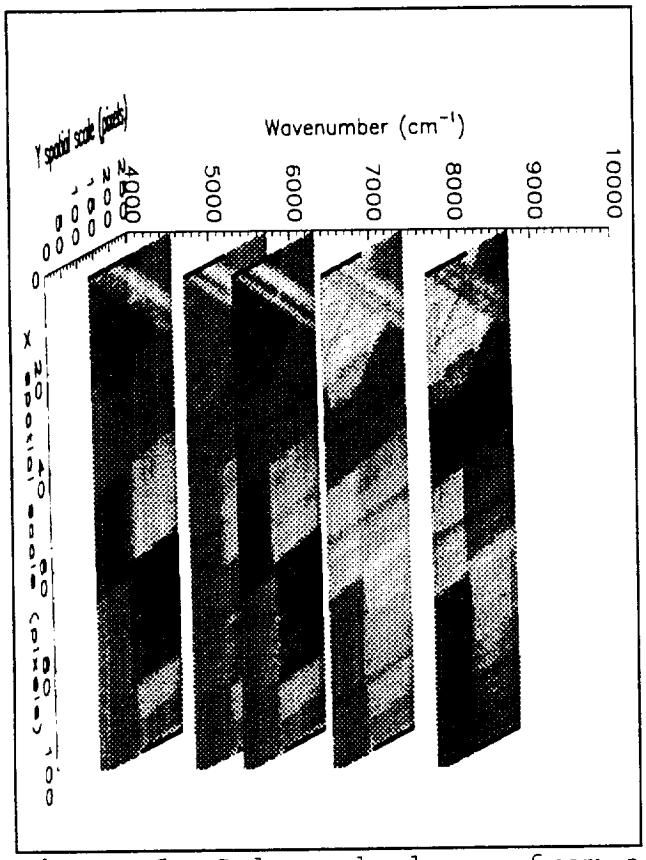

Figure 6. Selected planes from a DASI hyperspectrum of a NASA airstrip and surrounding fields.

a cross-track angular resolution of 0.5 mrad (= instantaneous field of view (IFOV)) over a 7.8° FOV. The hyperspectra are reconstructed from a time series of interferogram frames. The data represents the complete spectral/spatial characteristics of the field of view at time of observation. A plot of selected images from another hyperspectrum, obtained in this same C130 flight, is shown in Figure 6, where the spectral variations with wavenumber and with spatial position are defined by the spectral contrasts provided by CH absorptions and other spectral features of atmospheric, biological, and geological components.

S/N Considerations

Fourier transform spectrometers (FTS) superimpose N spectral elements onto the detector simultaneously, i.e. the signal is multiplexed (Felgett, 1951). An array detector must be capable of handling the large dynamic range signals provided by DASI. The large dynamic range for existing array detectors (e.g. 12 bits at 35 Hz frame rates) is adequate to provide an high S/N in DASI spectra.

Smith and Smith (1994) have given the relationship between the S/N in the interferogram and the spectrum, in agreement with experiment (see Brault, 1985 for a similar development). Since array frames can be flat fielded at or near the photon noise limit (see Kuhn et al., 1991, McLean et al., 1989), a S/N exceeding 500 may be expected for **single pixel rows** for arrays with charge wells exceeding 10^6 electrons. Smith and Smith (1994) show that the S/N of DASI spectra is optimized by observing only the spectral elements required for a specific science goal, consistent with the two-beam interferometer nature of DASI. This is accomplished by delimiting the spectrum with a bandpass filter or by the detector response, atmospheric transmission, and/or source spectral distribution.

Basically, the DASI's throughput advantage compared with an equivalent aperture grating monochromator allows a DASI to achieve a spectral resolution equal to a grating monochromator for the same acceptance angle (IFOV), Ω, while requiring a greatly decreased aperture, A, to pass the flux to the detector from the telescope. Conversely, weak signals like fluorescence or phosphorescence may be detected with DASI at a greatly increased S/N compared to prior measurements since a much larger flux can be made to reach the detector by either a propitious choice of telescope or FOV. At the same time, a physically much smaller DASI, compared with a grating monochromator, can be utilized for the measurements. This characteristic lends itself to the construction of small, stable hyperspectral imagers such as that we have proposed for the Pluto Fast Flyby (see below).

Figure 7. DASI hyperspectra mean wavelength (1.6 μm) image of cirrus clouds. The bar represents the region plotted in Figure 8.

DASIs can observe sunlight reflected or scattered from the scene of interest or emitted fluxes, for DASIs designed to operate into the MWIR and LWIR. Hence, the detector must be capable of handling large dynamic range signals. The HCT arrays we have used for DASI hyperspectra exhibit read noise characteristics and well depths that permit acquisition of photon-noise limited interferograms. The detector dynamic range needed for the study of broadband absorption spectra is available provided sufficient photons are detected. As described by Smith and Smith (1994), the S/N of DASI spectra is optimized by observing only the spectral elements required for a specific science goal.

DATA PROCESSING-DATA PRODUCT

Figure 7 is a mean wavelength spectral image obtained with a DASI for a cirrus cloud, similar to the mean spectral image in Figure 2. Figure 8 plots the water and ice scattering spectral features and flux contours between 1.2 and 2.2 μm. That such a spectral data set includes 100 or more spectral data points for every single point in the observed area underscores the fact that spectral data acquisition for a large surface region, its subsequent reduction and processing into a useable data product must be a systematic process that is highly automated.

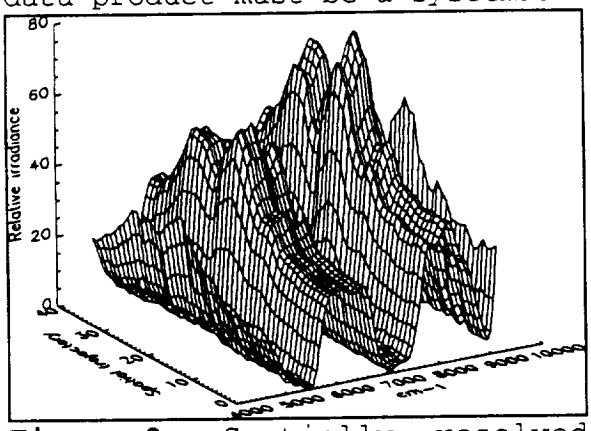

Figure 8. Spatially resolved spectra for the bar drawn on Figure 7.

Telescopic Tests of DASIs

In August, 1991, we took the DASI to Mauna Kea Observatory, but had bad weather as a passing hurricane blanked us out for the five day run. We succeeded in the acquisition of hyperspectra in December, 1992 for Mars, Venus and Jupiter from 0.4 to 2.2 μm, as well as spatially diffuse objects such as the Orion Nebula. The 0.6 meter telescope we used lacked accurate off-set capabilities so the hyperspectra are relatively coarse in the cross-track resolution.

Progress in DASI Applications to Space Science Missions

We have developed detailed space missions for DASIs as a major part of this program. The following concepts have been developed.

1. The PI in collaboration with Ball Aerospace presented a detailed concept for a Lumis Scout mission.

2. We developed a DASI infrared hyperspectral imager concept for a Mars panoramic camera and for μ-rovers.

3. The PI developed a novel concept that uses a DASI for the measurement of the composition of interplanetary (interstellar) dust particles (IDP), including the light elements normally not detected. This is a very low weight and data rate, passive experiment described in more detail below.

The concept entails the use of the extremely large field of view of a DASI to observe the plasma produced as an IDP transits a thin foil at an a priori unknown position. The plasma yields emission spectra of IDP constituents. Since a DASI requires no moving parts, an IDP DASI can wait passively for an IDP passage to trigger the selection of an interferogram from a linear array detector. The array is continually readout so that every incident particle's spectrum will be captured. Fast read rates and short integrations mean that no cooling is required. HgCdTe and Si arrays would provide spectral information from 120 nm to 2.5 μm. The application of DASIs to the study of IDP composition is absolutely unique in that no other instrument has both the large field of view, low weight, power, and high stability required for the determination of the composition of random incident IDPs. Clearly, the ability to determine the composition of dust throughout the solar system would greatly add to our knowledge of the heterogeneity as well as the abundances of the elements of the solar nebula.

4. As a continuation of this program, we were selected to develop an instrument design meeting the science measurement requirements of the Pluto Fast-Flyby mission. The envelope of the resulting DASI compared with the dimensions of the telescope illustrate the light handling capability of the DASI (see below).

DASI PARAMETER GOALS

A wide range of parameters has been discussed in the literature for remote sensing measurements of geochemical systems depending upon, for example, what objects are observed at what wavenumbers. We have made a selection of parameters for the measurement requirements for geochemical remote sensing as discussed below. The DASI is designed to the selected parameter set, but in fact is quite flexible. That is, the components are capable of easy replacement so that different spatial or spectral resolution can be selected. It is expected, however, that the parameters chosen will answer many requirements. The array detectors, the most important of the component devices in DASI, have only a fairly narrow range of characteristics. Once the detector selection is made, the remaining components must be then designed to match the measurement requirements to the array characteristics.

Detector Selection

The measurement parameters require specific detector characteristics. First, the detector must be capable of read rates in excess of 10 Hz. Higher read rates are desirable to allow the DASI's use at higher spatial resolution from the same platform or for multiple samples within

a spatial resolution element to enhance S/N. Second, the array must have high quantum efficiency across the required spectral region and low read noise and dark current. Third, the well depth per pixel for the array must be large enough that a photon noise limited response at adequate S/N can be achieved in the desired spectral regions.

SIGNAL-TO-NOISE RELATIONSHIPS

The attained S/N is a function of the flux brought to the detector within the allowed integration time, the spectral resolving power, the nature of the spectrum, the instrument function of the measuring instrument, the efficiency of its detection, and the sources of noise that confuse the signal (see Smith and Smith, 1994 and Brault, 1985 for a detailed discussion). The S/N also depends upon the adequate calibration of the array so that the data reach the photon shot noise limit rather than be limited by pixel-to-pixel variations of the array.

A DASI achieves S/N in the transformed spectrum $(S/N)_s$, compared with the S/N in the measured interferogram $(S/N)_i$, that is defined as follows (Smith and Smith (1994):

$$(S/N)_s/(S/N)_i = (B_t/BD) \times (N/2)^{-1/2}$$

In this equation, B_t/BD is the ratio of the total spectral interval sampled from 0 cm^{-1} to σ_{max} cm^{-1}, B_t, to the spectral interval, weighted with the actual detected spectral power, B, including the transmittance of the optics and the atmosphere or scatterers, etc. and multiplied by the response function of the detector, all from 0 to σ_{max} cm^{-1}, D. This recognizes that the interferogram noise is redistributed by the Fourier transform evenly over the entire spectral interval (Bracewell, 1965), including the regions where we know no signal exists or where the array is not sensitive. N/2 is the number of observed spectral samples, divided by two to account for the half of the noise in the interferogram in the imaginary part of the transform and is usually equal to the spectral resolution, R. The square of the S/N in the interferogram is simply the number of detected photons divided by the number of samples. This relationship clearly shows that as the resolving power is increased the spectral bandwidth is narrowed to maintain S/N in the transformed data.

Radiometric Analysis

Using the method described above, we present, in Table I, the parameters for a radiometric analysis of nominal SWIR and Vis-NIR DASI designs we have developed for inner solar system hyperspectra.

Table I

SWIR DASI Parameters (Designs for High Flux Case)

IFOV: 1.6 mrad, Ω: 2.56(e-6) str, FOV: 23.47°
Spectral Range: 0.85 to 2.5 μm Al=Albedo:0.3 X 1/π (Lambertian)
Optical Transmission of DASI;τ= 0.11 (lenses,polarizers,Wollaston)
Quantum efficiency: QE=0.65 (average over spectral range)
Telescope objective: aperture, 26.3 mm, focal length: 25 mm
Telescope area: A = 5.43 cm^2
Mean Flux for spectral range: F >2(10^{13}) Φ/sec/cm^2/cm^{-1} (H_2O included)
Bandwidth: B=7765 cm^{-1} Resolving power:R=125; 95 cm^{-1} @11,765 cm^{-1}
S/N(interferogram)= $[\sqrt{2FBATxQExAlx\Omega x\tau/R}]^{1/2}$ = 3.923(10^3)

Visible-NIR DASI Parameters

IFOV: 1.2 mrad, Ω: $1.44(10^{-6})$ str, FOV: 35.2°
Spectral Range: 400 nm to 900 nm Al=Albedo:0.3 X $1/\pi$ (Lambertian)
Optical Transmission of DASI; τ= 0.11 (lenses,polarizers,Wollaston)
Quantum efficiency: QE > 0.6 (average over spectral range)
Telescope objective: aperture, 26.3 mm, focal length: 25 mm
Telescope area: A = 5.43 cm^2
Mean Flux for spectral range: F >$2(10^{13})$ $\Phi/sec/cm^2/cm^{-1}$
Bandwidth: B=14,000 cm^{-1} Resolving power: R=125; 5.4 nm at 680 nm
S/N(interferogram)= $[\sqrt{2}FBATxQExAlx\Omega x\tau/R]^{1/2}$ = $3.325(10^3)$

note: well depth limits the S/N unless multiple frames are acquired.

The analysis shows that the SWIR DASI, for the assumed parameters, reaches a S/N well in excess of 500 (888 is calculated) for continuum regions of the incident solar spectrum for a spectral resolving power of 125. This resolving power is that of a two-beam interferometer, and should be multiplied by a factor of 2-3 to compare with a grating/prism monochromator resolving power. These calculations are carried out for 100 msec integrations for the specified IFOV. This requires a camera frame rate of 10 Hz that is readily achievable and compatible with feasible readout rates to the bulk data storage facility. Additional assumptions behind Table I are that observations are made of a Lambertian surface with a mean albedo of 0.3 from 0.85 μm to 2.5 μm.

The spatial resolution (IFOV) and the telescope collection area are coupled through the optical speed. We have designed DASIs as fast as f/0.95 with wide field optics. These optics allow the DASI to collect the high fluxes required to reach near full wells of 3×10^7 collected electrons for high temperature HgCdTe SWIR detectors and thus attain a very high S/N within the limited integration time. As shown in Table I, an increase of the FOV to even 34.5° is feasible. This last FOV will result in measurable loss of resolution near the field of view edges. It is presented to show that, while compromising spatial resolution near the edges of the FOV, a DASI can substantially exceed the angular aperture of any previously proposed imaging spectrometer with no loss of spectral fidelity. These fast designs are suited to use in the MWIR and LWIR since they can provide very large fluxes to the focal plane allowing the use of higher temperature focal plane arrays.

For the 40 μm pixels of the HgCdTe SWIR array, the DASI configuration must match the pixel dimension through the DASI to the IFOV. For example, the 0.8 mrad IFOV and the 40 μm pixel size require that the effective focal length of the telescope be 50 mm. A larger IFOV results in a nearly proportionally shorter focal length for the primary optic.

DASI DESIGNS

The LUMIS DASI optical design is plotted in Figure 9. The design allows for high signal-to-noise, spectral resolution, and spatial resolution. The polarizers for the SWIR are wire grid polarizers that show high throughput and efficiency for all incident wavelengths. The reflective telescope offers a wide FOV while maintaining achromaticity. This arrangement gives the DASI a wide FOV (up to 34°), achromatization over the detector spectral region, a flat focal plane, a small f/# without using obscured apertures, and most importantly a very high throughput so that the desired high S/N can be achieved.

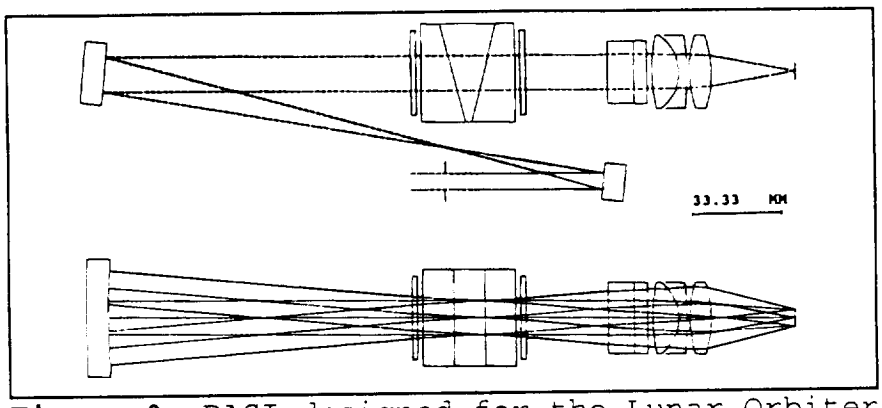

Figure 9. DASI designed for the Lunar Orbiter mission that permits high S/N hyperspectra to be acquired for the entire surface.

The PFF PRIMIS enclosure is drawn to scale in Figure 10. PRIMIS' envelope is dominated by the telescope rather than the DASI.

EFFECTS OF TEMPERATURE ON DASIs

The analysis of the spatially resolved interferograms requires consideration of the parameters that effect the spatial dependence of the interferogram. The frequency, σ_{max}, is affected by alterations in α. Correspondingly, the spectral resolution of $\delta\sigma$ is inversely a function

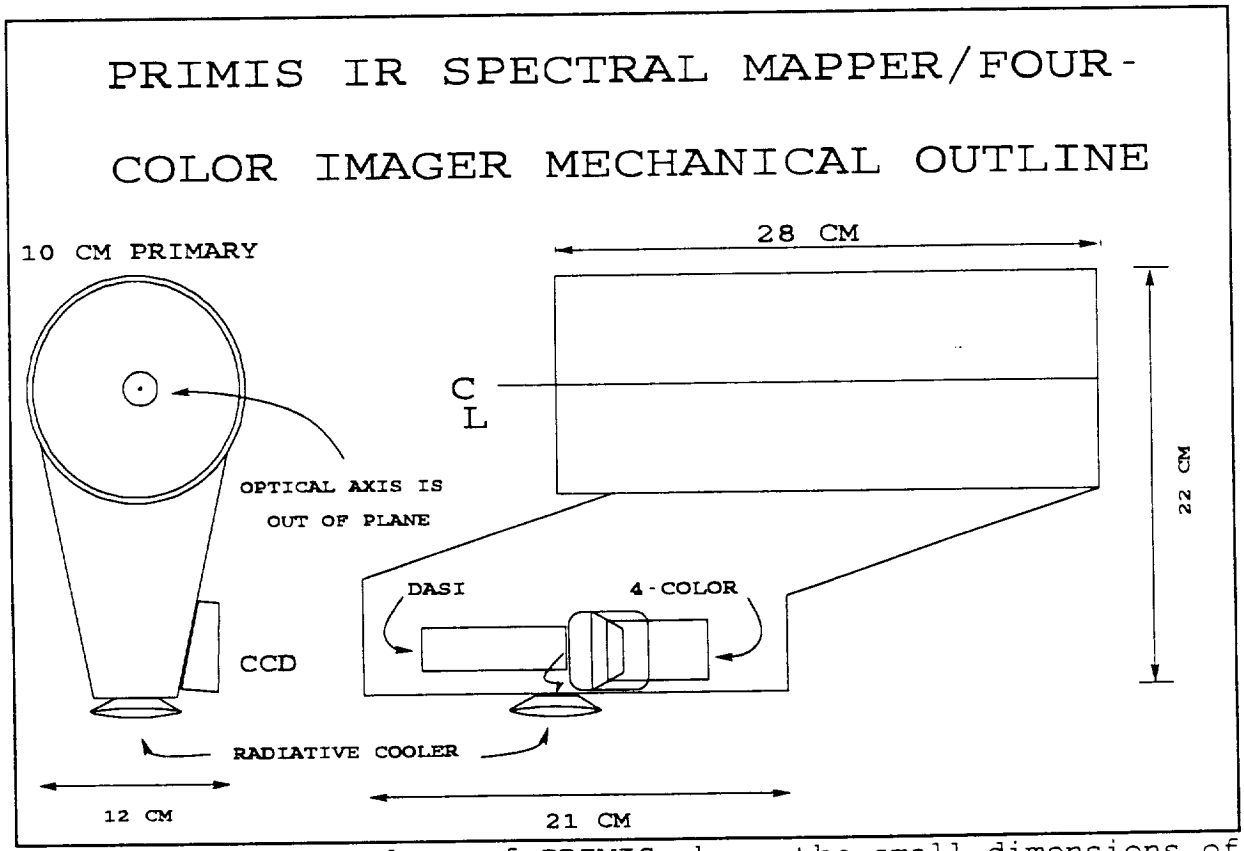

Figure 10. The envelope of PRIMIS shows the small dimensions of the DASI compared with the telescope, the reverse of most grating spectrograph designs.

of α. The shearing angle of a Wollaston is given by

$$\alpha = 2\ (n_o - n_e)\ \tan\ \Theta$$

where Θ is the cut angle, i.e., the angle between the outer and inner prism faces. The temperature dependence of the birefringence of magnesium fluoride, a suitable optical material for DASI's Wollaston prisms for use to beyond 7 μm, is required to evaluate the effect of temperature on DASI characteristics, all else being held constant. Dodge(1984) reports the temperature dependence of the MgF_2 birefringence which we shall consider here. In the wavelength range of interest for SWIR studies, from 0.4 to 2.5 μm, the temperature coefficient dn/dT for MgF_2 is $\leq 2 \times 10^{-6}$ $°C^{-1}$. The coefficient is slightly dispersive for the ordinary and extraordinary axes, The important quantity in the DASI context, $d\Delta n/dT$, is $< 5 \times 10^{-7}$ $°C^{-1}$ across the specified wavelength range.

Δn for MgF_2 is near 0.01 for the specified wavelength range so that the temperature coefficient, $d\Delta n/dT$, corresponds to less than 5×10^{-5} change in Δn $°C^{-1}$. In turn, the number of fringes sampled, e.g. 250 with a 500 element array, is changed by 1.25×10^{-3} fringes $°C^{-1}$.

The effects of temperature then are such that a ten degree temperature change would cause only an 1/8 th fringe shift across the entire array, a negligible error. The magnitude of these figures indicates that the dependence of birefringence on temperature is small enough to be ignored, even for a sudden 10 °C temperature change that occurred between spectral images. Further, since the temperature can (will) be measured, the wavelength/resolution correction of a particular measurement is determined by the known temperature dispersion of birefringence and can be allowed for in the analysis.

In addition, the wavenumber dependence of the indices of refraction may be modelled as a linear function of wavenumber for the SWIR. We have found that a linear model represents the dependence sufficiently well in that spectral region that higher order fits are not required to yield a sufficiently linearized wavenumber plot from FFT'd data.

Publications

1. Digital Array Scanned Interferometers, (with W. V. Schempp), Experimental Astronomy, 1, 389-405, 1991

2. Progress with IR Measurements with Digital Array Scanned Interferometers (DASIs),(with P. Hammer, A. Delamere, M. Duncan, and D. Dorn, Paper 34.10, presented at Division of Planetary Sciences Meeting, Nov., 1991

3. Remote Sensing of Earth's Atmosphere and Surface using a Digital Array Scanned Interferometer-A New Type of Imaging Spectrometer, J. Imaging Science, 36 417, 1992, (with P.D. Hammer and D.L. Peterson).

4. An Imaging Interferometer for Terrestrial Remote Sensing, (with Hammer, P.D., Peterson, P.D.), SPIE ,1937, 244 (1993)

5. Spectral Imaging of Clouds Using a Digital Array Scanned Interferometer, (with Hammer, P.D.) Atmospheric Research 34, 347 1994.

6. Digital Array Scanned Interferometers II. Figure of Merit Analysis., (with Smith, K. M.) to be submitted, Applied Spectroscopy, 1994.

SUMMARY

The hyperspectra results presented here demonstrate clearly that the DASI can perform hyperspectral measurements for a broad range of objects and environments now believed to be essential for progress in solar system atmospheric and geochemical studies, as well as Earth-oriented missions. DASIs, as described here, are shown to be stable, simple, high throughput, and efficient spectrometers that can acquire spatially resolved, low to high spectral resolution observations of extended or resolved sources. Suitable visible, SWIR, MWIR and LWIR array detectors are available to take advantage of these innovative devices for purposes of remote sensing in space borne applications.

Remote measurement of surface and atmospheric spatio-spectral characteristics from a space platform requires very high signal-to-noise spectra, routinely acquired and reduced to the desired parameters. Incident solar radiation traverses an atmosphere, containing clouds, aerosols and molecular absorbers, then reaches the surface of the land where it is transmitted, reflected, scattered, or absorbed. The returned radiation contains sufficient spectral information to derive the nature, present state, and temporal transitions underway among the components of the interacting atmospheric surface system. The problem is complex, but nonetheless, acquisition and processing of spectral information from remote sensing studies has shown that useful inferences can be made. Remote sensing methods and the interpretation of the returned data is rapidly evolving, but it is clear that high signal-to-noise, spatial, and spectral resolution are demanded from the data in order to separate the observed components. The DASI will permit acquisition of high quality spectral imaging of biological systems in the ocean and on the land. The requirements for increasingly sophisticated data coupled with a pressing need to keep instruments simple, reliable, inexpensive, and adaptive argue for the proposed DASI's construction since it is, from prior experience, an instrument that can be operated at modest cost.

REFERENCES

Bracewell, R., " The Fourier Transform and Its Applications", McGraw-Hill, 1965

Felgett, P., PhD thesis, Cambridge University, 1951.

Hammer, P.D., Peterson, P.D., and Smith, W.H., SPIE ,1937, 244 (1993)

Hammer, P.D. and Smith, W. H., Atmospheric Research 34, 347 1994.

Jacquinot, P., J. Opt.Soc.Am.,44, 761,(1954)

Kuhn, J. R., H. Lin, and D. Loranz, P.A.S.P., 103, 1097 (1991).

McLean, I. S., Casali, M. M., Wright, G. S. and Aspin, C., in Proc. 3rd Infrared Detector Technology Workshop, NASA TM-102209, p. 183-201, 1989.

Okamoto, T., S. Kawata and S. Minami, Appl. Spectrosc., 40, 691 (1986)

Ring, L. and Stephens, C. L., Mon. Not. R. Astr. Soc., 158, 5p, 1972.

Smith, W. H., Patent No. 4,976,542
Digital Array Scanned Interferometer, issued Dec. 11, 1990.

Smith, W. H. and Schempp, W., Experimental Astronomy, 1, 389, 1991.

Smith, W. H. and Smith, K. H., Digital Array Scanned Interferometers II. Figure of Merit Analysis., to be submitted, Applied Spectroscopy, 1994.